CREATE Lab Semester Project

Tracking falling objects with 6 DOFs using computer vision

Naël Dillenbourg, Robotics

21.06.2024

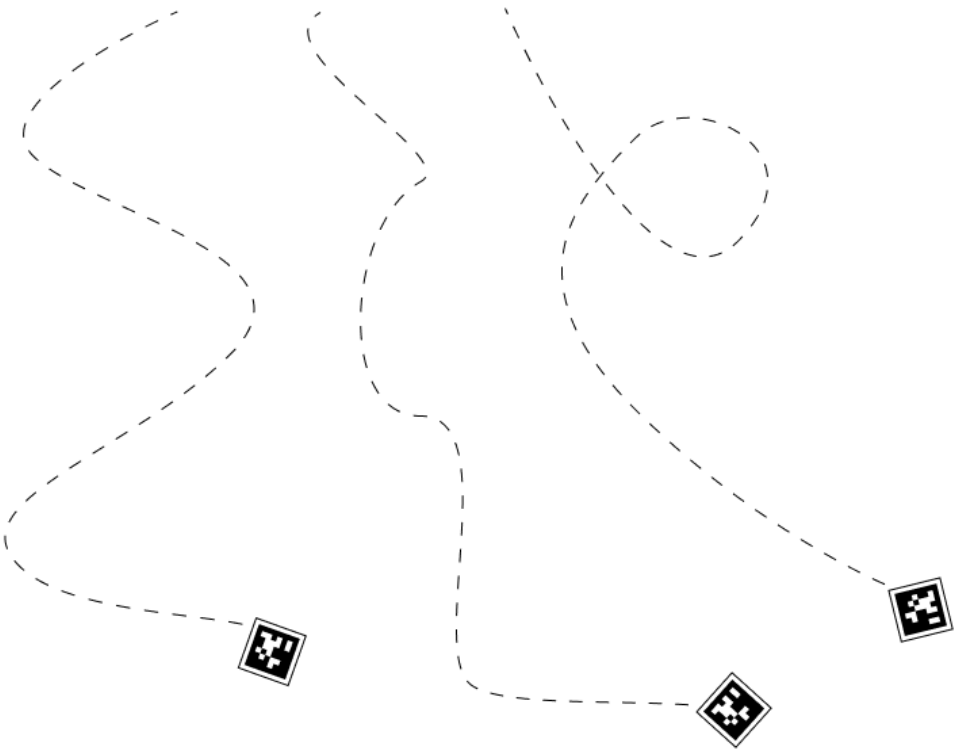

1 Introduction

1.1 The Falling paper project

The falling paper problem is a physics problem focused on the complex dynamics of paper as it falls through the air. The motion of a piece of paper is influenced by a large array of factors such as air resistance, shape, and weight distribution, resulting in various downward trajectories, unlike more straightforward free-falling objects.

For this project, we wish to be able to examine how different factors (such as shape, and size..) cause the paper to display different behaviors: such as fluttering, tumbling, or chaotic motion. For the falling paper problem, different tools have been developed to approach this problem. Some papers have a theoretical approach: using statistical mechanics and chaos theory. [1] [2]

Other studies employ advanced techniques such as computer vision and machine learning to analyze the motion of falling paper. These approaches allow for large-scale experiments and more precise classification of the motion patterns, which should help build a deeper understanding of the physics involved.[3] [4] [5] [6]

1.2 Large-scale experiments

The falling paper problem offers an interesting look at complex problems that mix aerodynamics, physics, and chaotic systems. This problem examines how flat objects, such as sheets of paper, descend through the air. The results vary with a large array of motions ranging from simple fluttering to unpredictable chaotic paths. Being able to conduct large-scale experiments on this problem provides valuable insights into the key features determining these motions and has applications in various scientific and engineering fields.

A large-scale experimentation on the falling paper problem was seen as an interesting approach as it has some interesting advantages:

- Statistical Significance: Having a setup usable to observe a large number of paper falls, should enable us to gather statistically significant data, and make robust conclusions about the general behaviors. This approach mitigates the variability inherent in small-scale experimentation and should allow for the identification of consistent patterns.
- Diverse Conditions: Large-scale experiments should allow for the investigation of a wide range of variables, such as different paper shapes, sizes, weights, and initial conditions. This diversity should help us understand how each factor influences the paper's descent.
- Advanced Analysis Techniques: Utilizing modern tools like high-speed cameras, computer vision, and machine learning algorithms, we should be able to numerically capture and analyze the motion of the falling paper.

2 Methods

This project focused on the creation of an experimental setup to test the feasibility of 6 Degrees of Freedom (DoF) analysis using QR codes.

In order to capture most of the trajectory, the paper has a tag on each side and is captured by three different cameras with varying angles.

We attempted to build a reliable setup based on Apritag markers that could capture the 6 Dof of a falling paper. [7].

To do this analysis, several steps were along the road:

- Checking existing literature: The first step was understanding what was already attempted, what was missing in these attempts, and the previous experiment setups built.

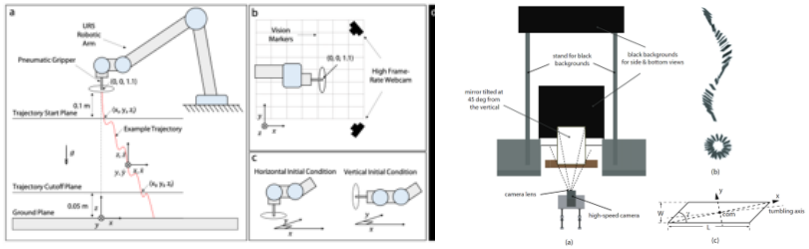

(a) Setup from [3] (b) Setup from [4]

Figure 1: Paper falling experimental setup used in litterature

- Using tags for 3d position calculation meant also checking what was already done in this field and the limitations. We used Apriltag instead of Arcuo markers due to the detection process being less computationally heavy.
- Building prototype of paper tracking: From there we built a 2d tracking prototype. This enabled us the get familiar with the tracking process.
- Working paper tacking: Expending to 3d position calculation using pose estimation algorithm allowed us to take this project to the next step.

Figure 2: Pipeline of the analysis

- Code to run the experiment: Controlling several cameras, syncing the tracks, dropping a paper, recording and organizing files for a large scale.

Figure 3: Pipeline of the experiment

- Fine-tuning the code: This part was the most time-consuming. As we had to fine-tune some parts of the pipeline to get better results, to redefine the pose estimate algorithm (chapter 3.1) to switch paper types to reduce deformation (chapter 5.1).
- Running experiments: Once this was done, it was still necessary to run experiments using various shapes to validate the experiment setup.

3 Experiment Setup

The setup consists of three cameras, a falling double-sided tag, a reference tag, and a grabber/dropper for repeatability. The dimensions are in available in figure 14.

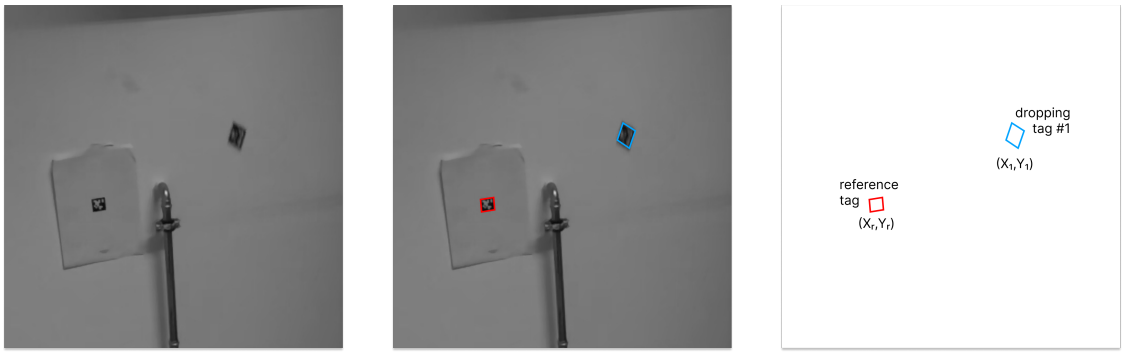

Figure 4: Detected tags example

3.1 Pose estimation

First capturing each frame, we detect the edges of all visible corners. Using this information we use an algorithm to extract the translation and rotation matrix of the tag from the camera's reference. For this, we attempted to compare different algorithms, using non-linear Levenberg-Marquardt minimization scheme[8], Complete Solution Classification for the Perspective-Three-Point Problem[9], Efficient Perspective-n-Point Camera Pose Estimation [10] and many more. Through an experimental comparison 5, we concluded that non-linear Levenberg-Marquardt minimization scheme[8] produced minimal reproduction error.

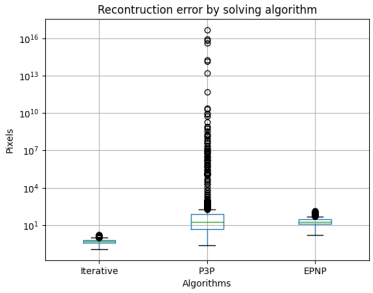

Figure 5: Reconstruction error for different algorithms

We also refine our calculated coordinates using a Gauss-Newton non-linear minimization scheme[11]. This should further improve accuracy as it attempts to minimize reconstruction error.

We were unable to use a robust line segment matching approach based on lbd descriptor and pairwise geometric consistency[12], as it was unable to fit the projection on most of the frames.

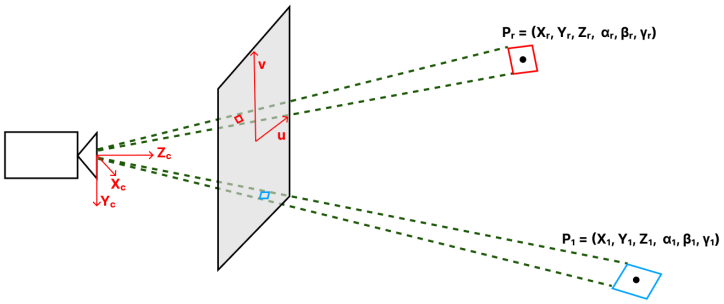

Figure 6: Position Calculation Schematics

From the calculated translation and rotation matrix, we then handle coordinate transformation to obtain the trajectory.

3.2 Coordinate Transformation

As we do not have a robust setup with a defined distance and angle between cameras, calculating relative coordinates is a difficult step as it has consequences on the precision of the experiment.

We opted to add a reference QR code that is seen by all cameras on the setup, this enables us to move the cameras around and maintain an accurate reference position. This means no need for a permanent setup with strictly defined distances between cameras.

Figure 7: Translation vector calculation

As the camera captures the position and runs a pose estimation algorithm (chapter 3.1). From there we extract a translation vector (figure 7) and a rotation vector describing the position and rotation of the camera in the tag's reference. From there, we can get the position and rotation of the falling tag in the frame of the reference tag.

$$\begin{bmatrix} X \\ Y \\ Z \end{bmatrix} = R_r^T \times (T_{1-2} - Tr) \tag{1}$$

1: Position calculation formula

Index r is the reference matrix, index 1-2 is the tag 1 or 2 depending on which one is visible.

$$R = R_{1-2}^T \times R_r \tag{2}$$

2: Rotation matrix calculation

$$\begin{aligned} \psi &= \arctan 2(\frac{R_{10}}{cos(\theta)}, \frac{R_{00}}{cos(\theta)}) \\ \theta &= \arcsin(-R_{20}) \\ \phi &= \arctan 2(R_{21}, R_{22}) \end{aligned} \tag{3}$$

3: Angles calculation.[13]

We should note that using Euler to calculate the angles may lead to selecting the wrong angles as the equations may have several solutions. But the information we obtain is enough to have an educated guess at the trajectory type.

3.3 Dropping mechanism

The dropping mechanism relies on an Arduino connected to a servo motor with a 3D-printed claw. This allow for a setup with more reproducible as the height is controlled by this mechanism.

However, this method while enabling some reproducibility does not ensure full control over the initial conditions. We observed that the dropping angle does vary from drops to drops and we know that such a variable may lead to drastically different trajectory changes.

We recommend switching to a faster mechanism, one that has less or no consequence on the trajectory based on the opening trajectory of the claws. Using a pneumatic Gripper as it was done in some large-scale paper falling experiments seems to be a better fit.[3]

As we mention further in the report, we believe the dropping mechanism does have a large effect on the trajectory: often forcing a tumbling motion due to the opening path of the claw.

3.4 Cameras

For this setup, we started with two cameras but ended up moving to 3. Finding the right framerate was crucial, as a too-low framerate does not allow for enough data points to be captured to construct a trajectory but higher framerates mean more data to analyze and longer computing times. The same is true of using high-definition images. We ended up using 3 GoPro Cameras recording at 2.7K 240 frames per second.

The distances between the dropped image, the reference tag, and the camera were also found to be a factor in the success of the experiment. Recording from too far away or too close does not enable the software to detect the tag especially if we wish to use small tags. Also, putting the camera too close to the falling tag means covering less of the trajectory and needing to divide the trajectory per camera, which removes some needed redundancy.

However, our setup and code enable us to easily add cameras without limit. This is at the cost of computation time as more data needs to be processed for the trajectory computation.

A major benefit of our setup is its low-cost feasibility. High-frame cameras, storage space and servers to extract the data may cost a lot. This solution is compatible with a lower budget and can be run using consumer cameras and a laptop.

4 Results

We selected a few paper shapes to test the setup built. We focused on testing the setup using examples used in related literature [3].

The addition we make with this setup is tracking the 6 degrees of freedom from a falling paper instead of the three degrees of freedom tracked in most attempts. While this project does not establish the importance of some hyper-parameters in determining the trajectory type, we hope that proving the feasibility of this method allows for more research to be done.

We plotted some example results using different shapes and added the plots in the annex.

- An hexagonal following a tumbling trajectory: Figure 10.
- A square following a tumbling trajectory: Figure 11.
- A cross following a tumbling trajectory: Figure 12.
- A circle following a tumbling trajectory: Figure 13.

Animated versions of these plots with the corresponding camera frame are available on the gitlab repository.

Some trajectories are however easier to capture. We found the tumbling trajectory especially hard as the falling paper's angle with regard to the camera makes the image often unreadable as we can observe in figure 8.

(a) Readable QR code (b) Unreadable QR code

Figure 8: Readability issue due to paper angle

The problem is however not easily fixed by switching cameras as they are unable to cover all angles for the whole trajectory.

We can also add that in the vast majority of cases we observed tumbling trajectories. We explain this due to the initial falling condition, and the setup of the dropping that forced this tumbling motion. 3.3 .

5 Discussion

5.1 Paper deformation

Tracking the paper using a QR code has an additional major drawback. Using a QR code for pose estimation on an easily deformable paper can produce a faulty trajectory. This did seem to produce errors with the pose estimate switching rapidly between two trajectories. For this issue, we found no easy fix but changing the grammage of the paper used contributes to a more rigid falling body, deforming less and reducing errors. However, this does not solve the initial problem. This is an intrinsic issue with the method of corner pose estimation on a flexible body using printed markers.

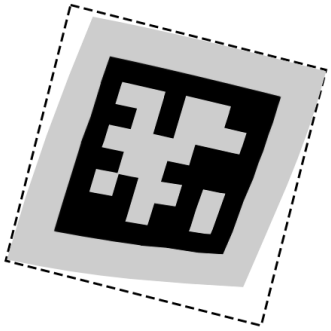

Figure 9: Deformed falling QR code

However, we could calculate the impact of the deformation by adding a mesh grid on the paper. This could in theory allow us to take into account the bending during the fall.

6 Conclusion

In conclusion, our project on tracking falling paper with six degrees of freedom using computer vision has demonstrated the feasibility of this method for tracking but advancements still need to be made to use it for understanding the complex dynamics of free-falling objects. By implementing a robust experimental setup with Apriltag markers and multiple cameras, we successfully captured detailed motion data for some typical trajectories. This should allow researchers to explore the influence of various factors such as shape, size, and weight on the paper's trajectory, thereby hopefully contributing valuable insights to the field of aerodynamics and chaotic systems.

Our experiments revealed that while QR code tracking on deformable paper introduces some inaccuracies, these can be mitigated by using more rigid paper or other techniques. Despite some limitations, the low-cost and adaptable nature of our setup provides a practical solution for large-scale experiments, enabling extensive data collection and analysis.

The results obtained from different paper shapes have shown diverse trajectory behaviors, emphasizing the limitations of the methods. Future work should focus on improving the dropping mechanism for better reproducibility and exploring advanced computational methods to enhance trajectory prediction accuracy.

Overall, our experiment setup lays a first foundation for future investigations into the falling paper problem using QR code pose-estimation, encouraging the use of advanced technologies and large-scale experimentation to unlock deeper understandings of complex physical phenomena.

References

[1] U. Pesavento and Z. J. Wang, "Falling paper: Navier-stokes solutions, model of fluid forces, and center of mass elevation," *Physical review letters*, vol. 93, no. 14, p. 144 501, 2004.

[2] Y. Tanabe and K. Kaneko, "Behavior of a falling paper," *Physical Review Letters*, vol. 73, no. 10, p. 1372, 1994.

[3] T. Howison, J. Hughes, and F. Iida, "Large-scale automated investigation of free-falling paper shapes via iterative physical experimentation," *Nature Machine Intelligence*, vol. 2, no. 1, pp. 68–75, 2020.

[4] K. Varshney, S. Chang, and Z. J. Wang, "Unsteady aerodynamic forces and torques on falling parallelograms in coupled tumbling-helical motions," *Physical Review E*, vol. 87, no. 5, p. 053 021, 2013.

[5] A. A. Pessa, M. Perc, and H. V. Ribeiro, "Clustering free-falling paper motion with complexity and entropy," *Europhysics Letters*, vol. 138, no. 3, p. 30 003, 2022.

[6] T. Howison, J. Hughes, F. Giardina, and F. Iida, "Physics driven behavioural clustering of free-falling paper shapes," *PloS one*, vol. 14, no. 6, e0217997, 2019.

[7] *GitHub - duckietown/lib-dt-apriltags: Python bindings to the Apriltags library — github.com*, https://github.com/duckietown/dt-apriltags, [Accessed 17-05-2024].

[8] K. Madsen, H. B. Nielsen, and O. Tingleff, "Methods for non-linear least squares problems," 2004.

[9] X.-S. Gao, X.-R. Hou, J. Tang, and H.-F. Cheng, "Complete solution classification for the perspective-three-point problem," *IEEE transactions on pattern analysis and machine intelligence*, vol. 25, no. 8, pp. 930–943, 2003.

[10] V. Lepetit, F. Moreno-Noguer, and P. Fua, "Ep n p: An accurate o (n) solution to the p n p problem," *International journal of computer vision*, vol. 81, pp. 155–166, 2009.

[11] E. Marchand, H. Uchiyama, and F. Spindler, "Pose Estimation for Augmented Reality: A Hands-On Survey," *IEEE Transactions on Visualization and Computer Graphics*, vol. 22, no. 12, pp. 2633–2651, Dec. 2016. DOI: 10.1109/TVCG.2015.2513408. [Online]. Available: https://inria.hal.science/hal-01246370.

[12] L. Zhang and R. Koch, "An efficient and robust line segment matching approach based on lbd descriptor and pairwise geometric consistency," *Journal of visual communication and image representation*, vol. 24, no. 7, pp. 794–805, 2013.

[13] G. G. Slabaugh, "Computing euler angles from a rotation matrix," *Retrieved on August*, vol. 6, no. 2000, pp. 39–63, 1999.

A Appendix

A.1 Results

Different colors correspond to different cameras.

A.1.1 Hexagone Example

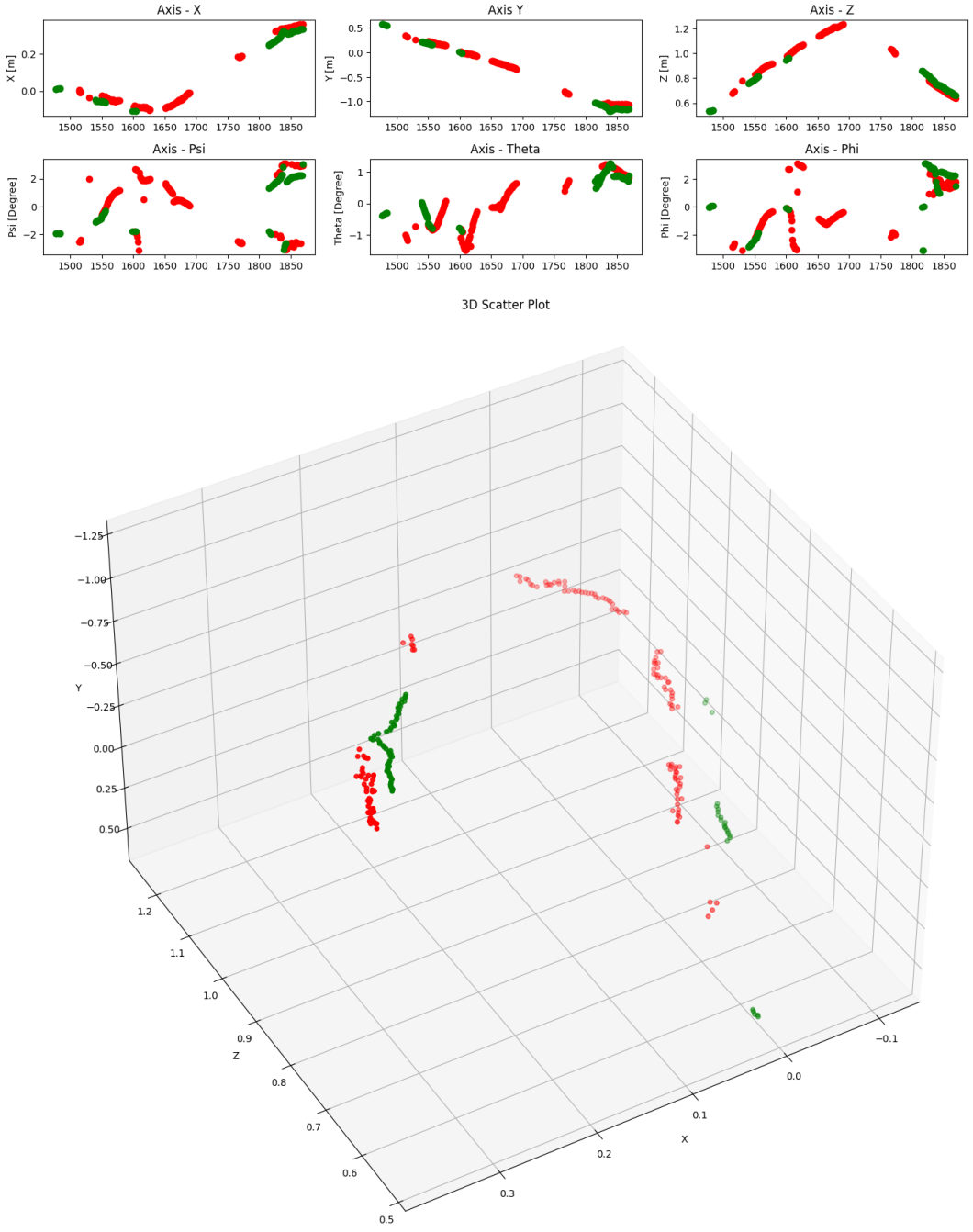

Figure 10: Fall of an hexagonal shaped paper

A.1.2 Square Example

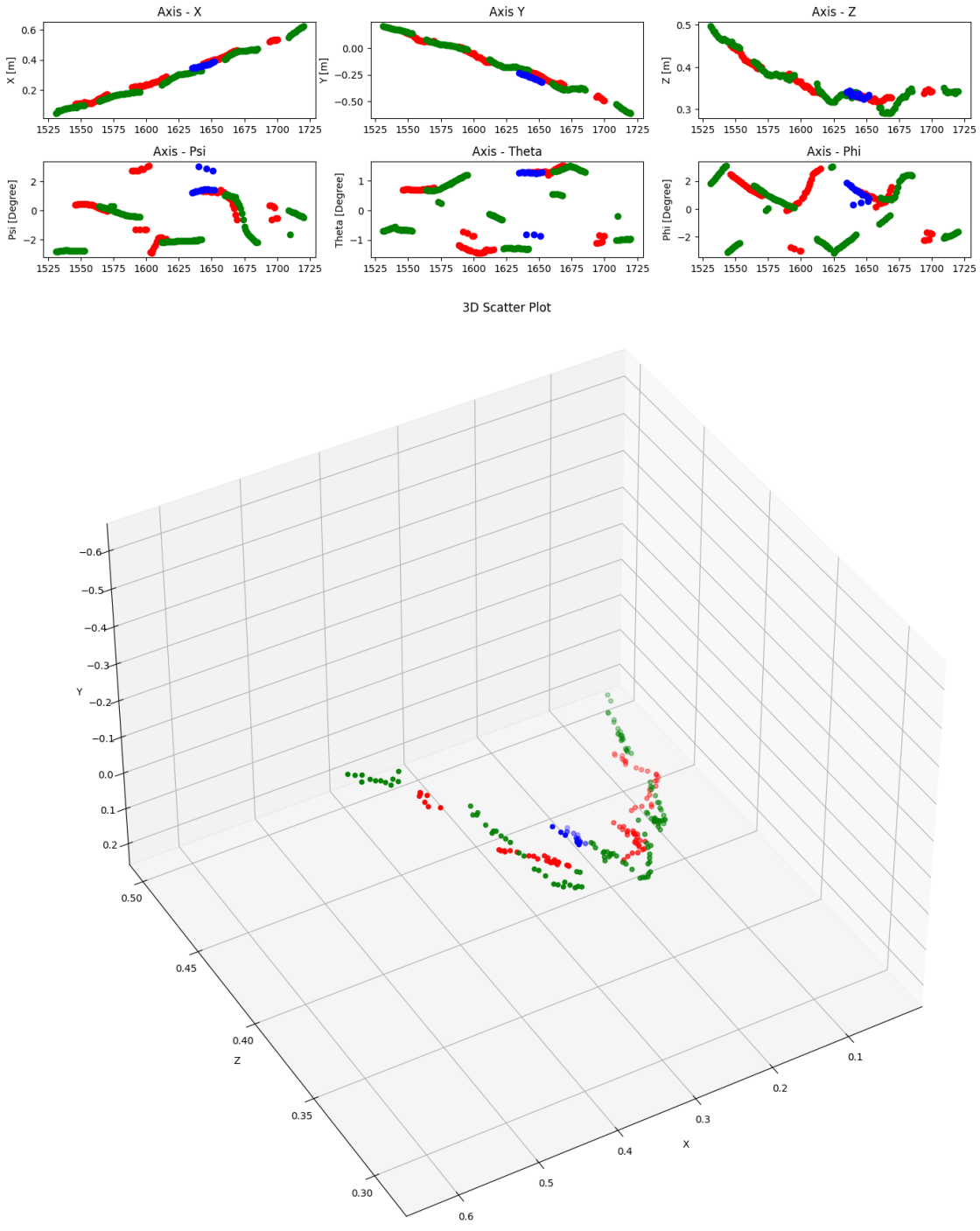

Figure 11: Fall of an square shaped paper

A.1.3 Cross Example

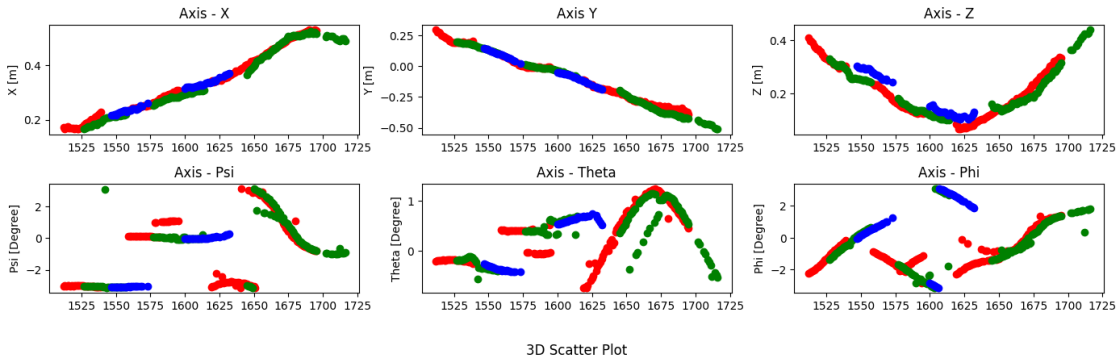

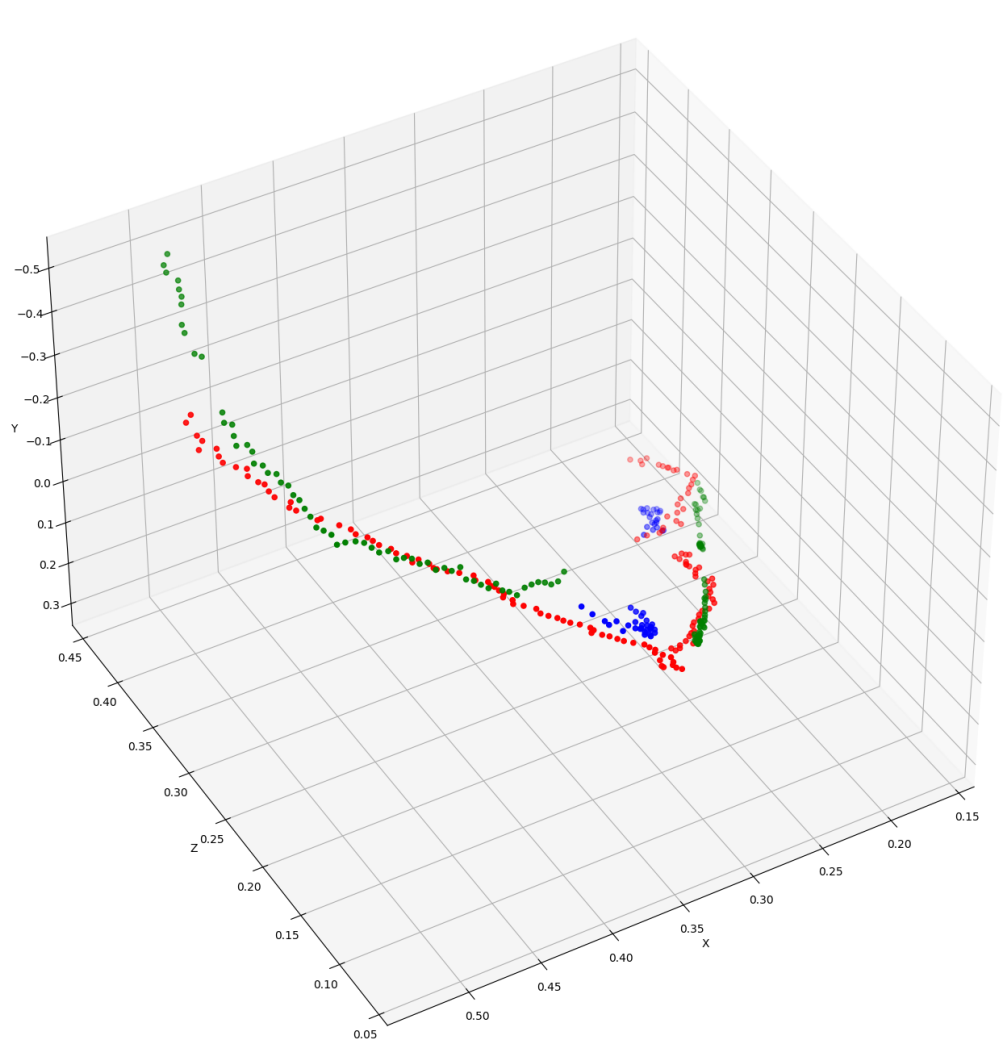

Figure 12: Fall of an cross shaped paper

A.1.4 Circle Example

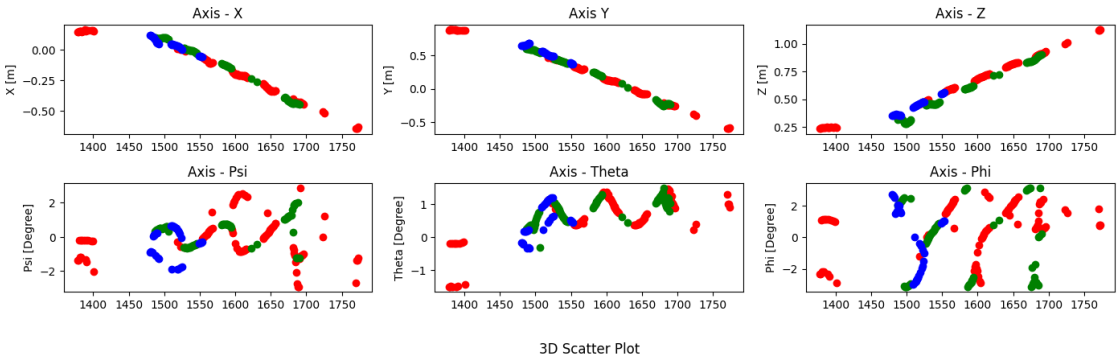

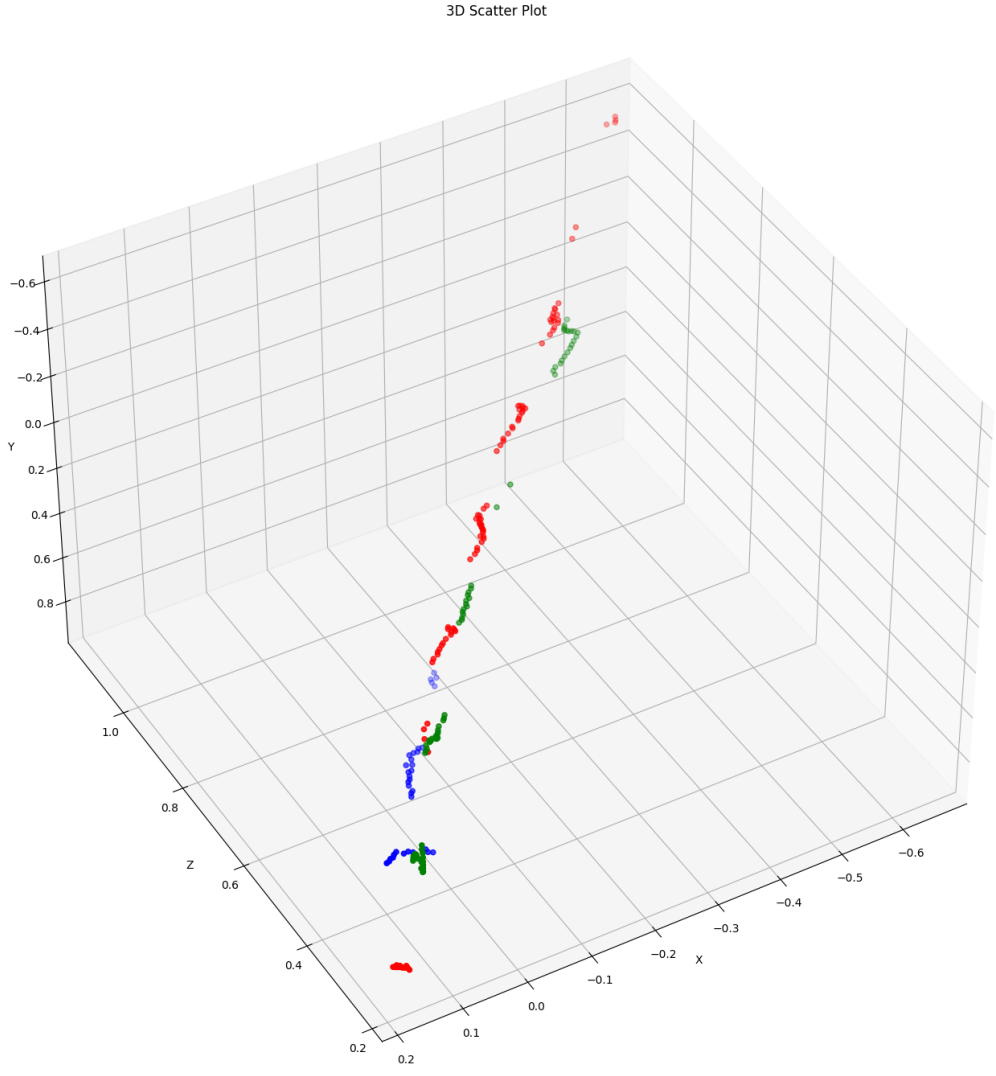

Figure 13: Fall of an circle shaped paper

A.1.5 Current setup dimensions

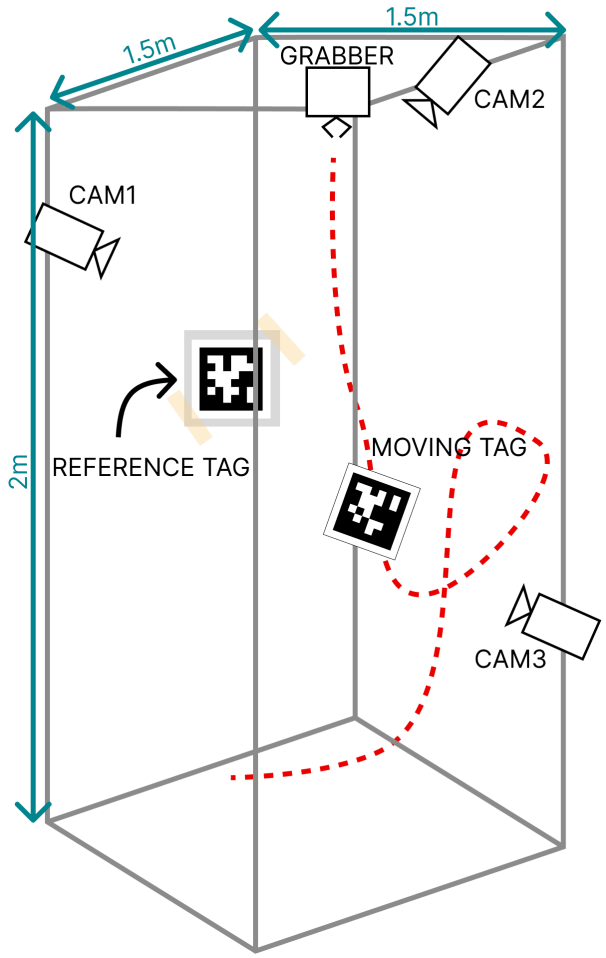

Figure 14: Experiment setup